Why Does a Man Post Rotator Cuff Repair Have Thoracic Outlet Syndrome and Pleural Effusions?

James D. Collins, MD

Keywords: radiology ■ anatomy ■ rotator cuff, pleural effusions ■ thoracic outlet syndrome ■ magnetic resonance imaging ■ brachial plexus

J Natl Med Assoc. 2011;103:284-292

Author Affiliations: University of California at Los Angeles, Department of Radiological Sciences, Los Angeles, California.
Correspondence: James D. Collins, MD, University of California at Los Angeles, Department of Radiological Sciences, 10833 Le Conte Ave, BL-428 CHS/UCLA mail code 172115, Los Angeles, CA 90095 (jamesc@mednet.ucla.edu).

CLINICAL HISTORY

The patient is a 51-year-old, right-handed male longshoreman with persistent right upper-extremity pain secondary to a fall from an equipment platform dropping 5 feet onto the pavement landing on his right shoulder. He felt instant sharp pain in the right shoulder and was immediately referred to a physician. His duties had included bending, stooping, squatting, standing, walking, pushing, pulling, and lifting upwards of 200 pounds. The examining physician took him off work and referred him to an orthopedic specialist. The orthopedist ordered magnetic resonance imaging (MRI) of his right shoulder, finding a right rotator cuff tear and recommending surgery. The surgery was performed repairing his right rotator cuff and biceps tendon.

PAST MEDICAL HISTORY

History of hypertension shows that blood pressure is under control. Basic metabolic panel 3 months prior to the MRI of his brachial plexus was within normal limits. The remaining history is otherwise unremarkable. Review of systems unremarkable except as above.

POSTSURGERY PHYSICAL EXAMINATION

The patient's blood pressure was 129/89 mm Hg; pulse, 69 beats/min; temperature, 98.6ºF; respiratory rate, 18 breaths/min. The cervical spine examination revealed bilateral trapezius muscle hypotonicity and tenderness; trigger points spasm of the paraspinal muscles and trapezius muscles; cervical spine range of motion and elbow and wrist examinations were within normal limits; upper extremities and his shoulder evaluation within normal limits save for positive impingement sign on the right; sensory examination of the upper extremities intact to pinwheel in all dermatomes and the upper extremity motor testing and upper extremity reflexes were also within normal limits.

DIAGNOSTIC IMPRESSION(S)

There was a complete right subscapularis muscle tear. The surgeon indicated the patient was in need of the definite repair of his torn right subscapularis muscle. In the meantime, he was to be maintained on present medications pending surgical procedure. The patient indicated he wanted a second opinion from his private physician.

Upon follow-up examination 1 month later with his primary physician, he presented with bilateral neck pain, right-sided numbness, severe headaches, sharp pain in his "frozen shoulder" and right thoracic outlet–like symptoms.[1] His physician indicated he should have a scalene muscle block and somatosensory evoked potential (SSEP) to determine whether he actually had the clinical diagnosis of thoracic outlet syndrome or not. The SSEP was recommended to rule out other complexity of etiologies. His physician proceeded to schedule him for the above tests with a neurologist. He also indicated he would see the patient after the tests were completed and make further recommendations. Both of the above tests were positive.

Because thoracic outlet syndrome was suspected, bilateral MRI/magnetic resonance angiography (MRA)/magnetic resonance venography (MRV) of the brachial plexus was requested to detect sites of brachial plexus compression.

Since the patient indicated he was claustrophobic and in extreme pain, he requested general anesthesia. His clinical history and physical examination recorded by the private physician were within the last 2 weeks and found acceptable for general anesthesia. His blood

pressure at the time of his MRI of the brachial plexus was recorded as 115/75 mm HG; pulse, 65; temperature, 98.4ºF; oxygen saturation, 99. He was then placed on the MRI gurney. Intravenous access was established with hyperextension of the head and neck to maintain his airway.

RADIOGRAPHIC AND MAGNETIC RESONANCE FINDINGS

The posterior-anterior chest radiograph (Figure 1) displayed the patient leaning left; asymmetric anterior-rotated heads of the clavicles over the posterior third ribs, right lower than left; decreased densities of the right soft tissues, subscapularis, serratus, deltoid, and pectoralis major and minor muscles reflecting the surgical repair site of the right rotator cuff and biceps tendon; low right first rib crossing the posterior second rib as compared to the higher left first rib; 2 metal densities with linear clip-like osseous extensions obscuring the medial head of the right humerus and the neck of right glenoid and the right deltoid muscle; mild right concave scoliosis of the cervicothoracic spine, C4-T5; retracted right hilum; hyperaerated lungs without flattening of the diaphragm, and normal cardiomediastinal structures. The lateral chest radiograph (not shown) displayed the arms extended forward, backward-displaced manubrium in close proximity to first ribs, bilateral round shoulders, normal cardiomediastinal structures, and hyperaerated lungs.

CONCLUSION(S)

- Post right rotator cuff and right biceps tendon repair.
- Soft-tissue defect over the right deltoid muscle, metal clips, and osseous density as above described.
- Atrophy of the right subscapularis, serratus, deltoid, latissimus dorsi, and pectoralis major and minor muscles.
- Bilateral round shoulders, right greater than left.[2]

The coronal sequence displayed the forward shift and mild compression of the soft tissues over the posterior neck and chest wall secondary to the rolled-up towel to maintain his airway; bilateral gray proton-dense edematous lungs and pleural effusions (Figure 2) matching the proton dense saline water bags on either side of the neck; hyperextension of the cervicothoracic spine; gray proton-dense scarring of the subcutaneous tissues over the right shoulder; mixed signal intensity artifacts (clips) marginating the glenoid labrum of the right shoulder (Figure 3); bilateral small internal jugular veins; compressed small right internal vein and the region of the right thoracic lymph duct; amorphous low signal defects within the body of the right glenoid and coracoid process as compared to the left shoulder; atrophy of the right deltoid, trapezius, serratus anterior, supraspinatus and infraspinatus muscles; high proton-dense fat-infiltrated atrophic subscapularis, infraspinatus, and the teres major and minor muscles; fracture deformity of the right acromion and the distal end of the right clavicle compressing the irregular gray proton-dense right suprascapular nerve; backward-displaced manubrium with the sternocleidomastoid muscles sloping posterior left placing the head of the right clavicle anterior to the left compressing the gray proton-dense thymus gland against the ascending aorta left of midline; gray proton-dense left brachiocephalic vein against the gray proton-dense brachiocephalic trunk giving common origin to the gray proton-dense left common carotid artery ascending anterior lateral accentuating the dilated gray proton-dense left subclavian artery ascending as the second division of the artery with binding nerve roots compressed posterior to the tense left anterior scalene muscle, backward displaced crimped (like a water hose) gray proton-dense right brachiocephalic artery (Figure 3, image 39); right clavicle with the subclavius and sternocleidomastoid muscles compressing the gray proton-dense right brachiocephalic vein and the inferior bicuspid valve within the small right internal jugular vein (Figure 3, image 41) against the right vertebral vein against the first division of the right subclavian artery, as compared to the dominant gray proton-dense left internal jugular vein; bulbous expanded gray proton-dense right subclavian vein on the low right first rib (Figure 3, image 41) as compared to the lower signal intensity of the bulbous

Figure 1. Posterior-anterior chest view displaying the forward-rotated right shoulder with metal clips/screws (X) over the right glenoid; fracture of the right acromion process (FX)

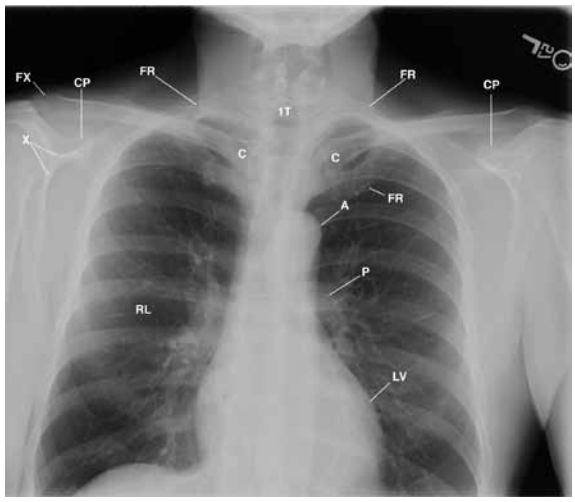

Observe the right arm (not labeled) in close proximity to the right chest wall as compared to the left arm.

A indicates aorta; C, clavicle (C); CP, coracoid process; 1T, first thoracic vertebra; FR, first rib; LV, left ventricle; P, pulmonary artery; RL, right lung.

expanded left subclavian vein on the high first rib; bilateral dilated gray proton-dense valveless anterior jugular veins diverting venous return from the junction of the compressed external jugular and subclavian veins on the first rib, right greater than left; gray proton-dense turbulent downward displaced left brachiocephalic vein reflecting impedance to venous return as the left brachiocephalic vein courses anterior to the splayed apart left common carotid artery and the crimped brachiocephalic artery as the left brachiocephalic vein joins the right brachiocephalic vein to form the superior vena cava, and electrocardiogram leads over the anterior chest wall.

The transverse sequence cross-referenced the coronal sequence to best display the gray proton-dense edematous lungs with dependent pleural effusions bilateral costoclavicular compression of the gray proton-dense subclavian veins, right greater than left (Figure 4A) and the manubrium sloping posterior left compressing the gray proton-dense turbulent left brachiocephalic vein against the ascending aorta and the gray proton-dense right brachiocephalic trunk with the left common carotid artery; gray proton-dense turbulent brachiocephalic vein reflecting impedance to arterial flow; elongated trachea reflecting the hyperextension of the cervicothoracic spine soft-tissue defect with multiple mixed-signal-intensity artifacts marginating the anterior atrophic right deltoid muscle and labrum from the head of the right humerus (Figure 4 A) with low signal defects within the body of the scapula and the coracoid process reflecting the surgery as above described; fat-infiltrated ischemic right subscapularis muscle as it courses anterior medial to the body of the glenoid, as compared to the left subscapularis muscle; head of the right clavicle anterior to the head of the left reflecting the manubrium sloping posterior left, small gray proton-dense right external jugular vein; costoclavicular compression of the inferior bicuspid valve within the internal jugular vein (Figure 4A) against the vertebral vein against the first division of the right subclavian artery; scarring of the resected right deltoid muscle involving the lateral supraclavicular nerves as compared to the left; mild costoclavicular compression of the bulbous expanded gray proton-dense left subclavian vein on the first rib accentuated by the costoclavicular compression of the dilated left axillary vein; irregular displaced soft tissues of the posterior chest wall secondary to the rolled-up towel as above described (Figures 4A and 4B); asymmetric sternocleidomastoid muscles compressing the internal jugular veins against the anterior scalene muscles, right greater than left (Figure 4B), diminishing venous return from within the smaller right internal jugular vein as it drains into the junction the gray proton-dense right subclavian and brachiocephalic veins.

Figure 2. Posterior coronal image displaying the hyperextension of the head (not labeled) and bilateral gray proton-dense pleural effusions (X).

A indicates aorta; LL, left lung; RL, right lung.

The transverse right and left oblique cross-referenced the coronal and transverse sequences. The sagittal sequence cross-referenced the coronal and transverse sequences to display the compressed soft tissues over the posterior chest wall, neck, and shoulder from the rolled-up towel placed to maintain the airway under general anesthesia; anterior-rotated clavicles with the sternocleidomastoid muscle compressing the inferior bicuspid valves within the internal jugular veins descending against the fascia of the gray proton-dense compressed first

division of the left and right subclavian arteries, right greater than left (Figure 5, images 38/94 and 56/98), gray proton-dense edematous left and right lungs with pleural effusions, (Figure 5 images 38/94-56/94; mild compression of the inferior bicuspid valve within the mixed low signal intensity of the left internal jugular vein as it drains into the gray proton-dense turbulent left brachiocephalic vein (Figure 5, image 38/94) as compared to the intermediate high proton-dense inferior bicuspid valve within the right internal vein (Figure 5, image 56/94).[3]

The 2-dimensional time-of-flight MRA/MRV stacked (not displayed) and 3-dimensional reconstructed coronal images without contrast confirmed the above. The 3-dimensional reconstructed coronal image (Figure 6) best displayed the backward-displaced head and neck as above described on the T1-weighted images; high-proton density of the superior sagittal sinus diverting high-proton-dense venous return within the transverse and sigmoid sinuses down into the dominant left internal jugular vein that is compressed by the sternocleidomastoid muscle displayed on the T1-weighted images above; high proton-dense first division of the left subclavian artery as it decreases signal intensity into the second division of the left subclavian artery; high proton-dense left external jugular vein as it decreases signal intensity into and over the left subclavian vein; high

Figure 3. Serial coronal images (38-41) of the right shoulder that display the metal staples within the head of the humerus (X); scar over the right deltoid muscle and the region of the right coracoid process (CP); costoclavicular compression of the inferior bicuspid valve within the right inferior internal jugular vein (J); costoclavicular compression of the gray proton-dense right subclavian vein (SV) and axillary artery (AX); crimping (like a water hose) of the brachiocephalic artery (BR) as it exits the aorta (A).

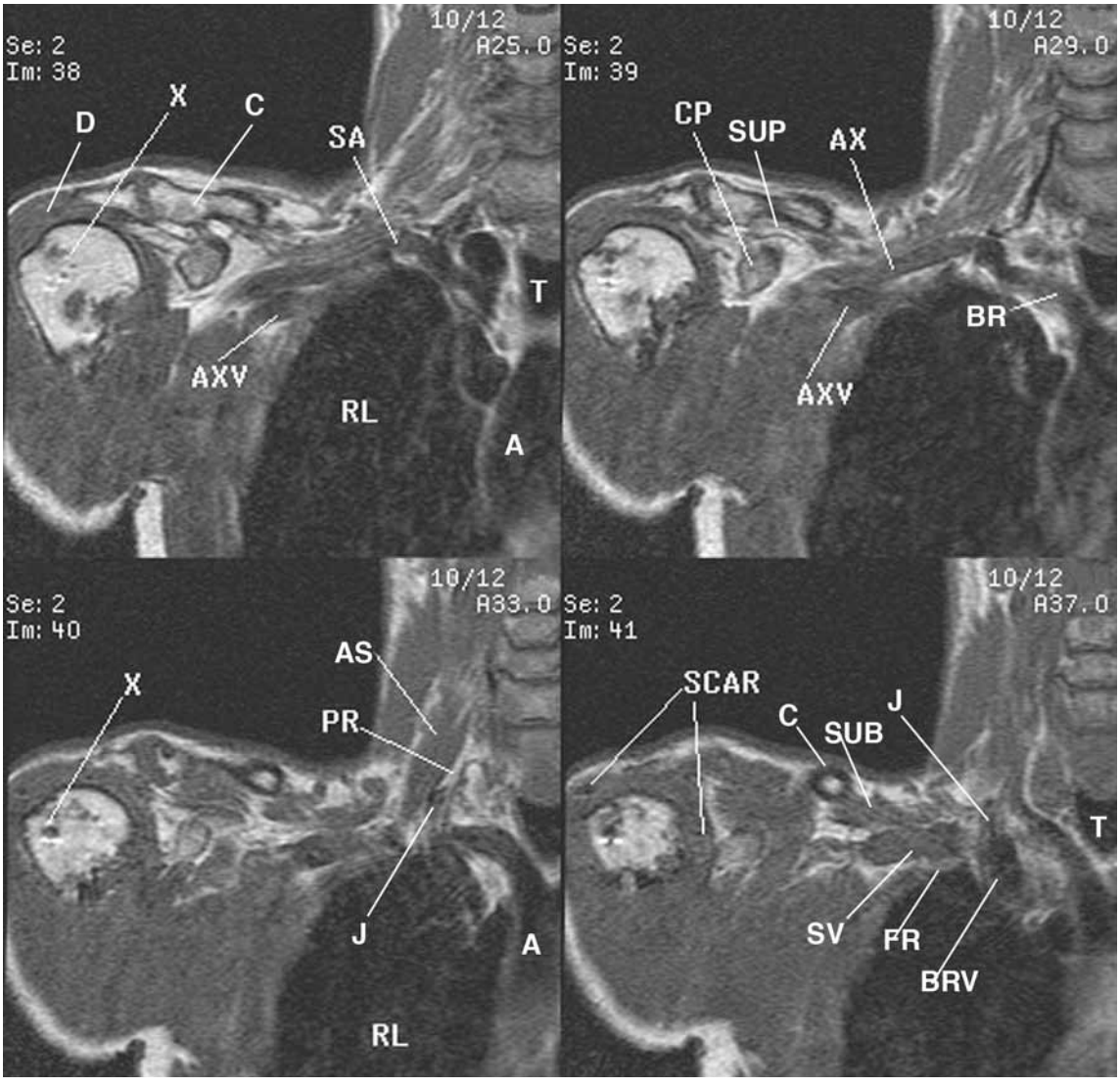

AS indicates anterior scalene muscle; AXV, axillary vein; BRV, brachiocephalic vein; C, clavicle; D, deltoid muscle; FR, first rib; PR, phrenic nerve; RL, right lung; SUB, subclavius muscle; SUP, suprascapular nerve; T, trachea.

Figure 4. Selected transverse images, 20/80 and 26/80, that cross-reference the T1-weighted coronal series

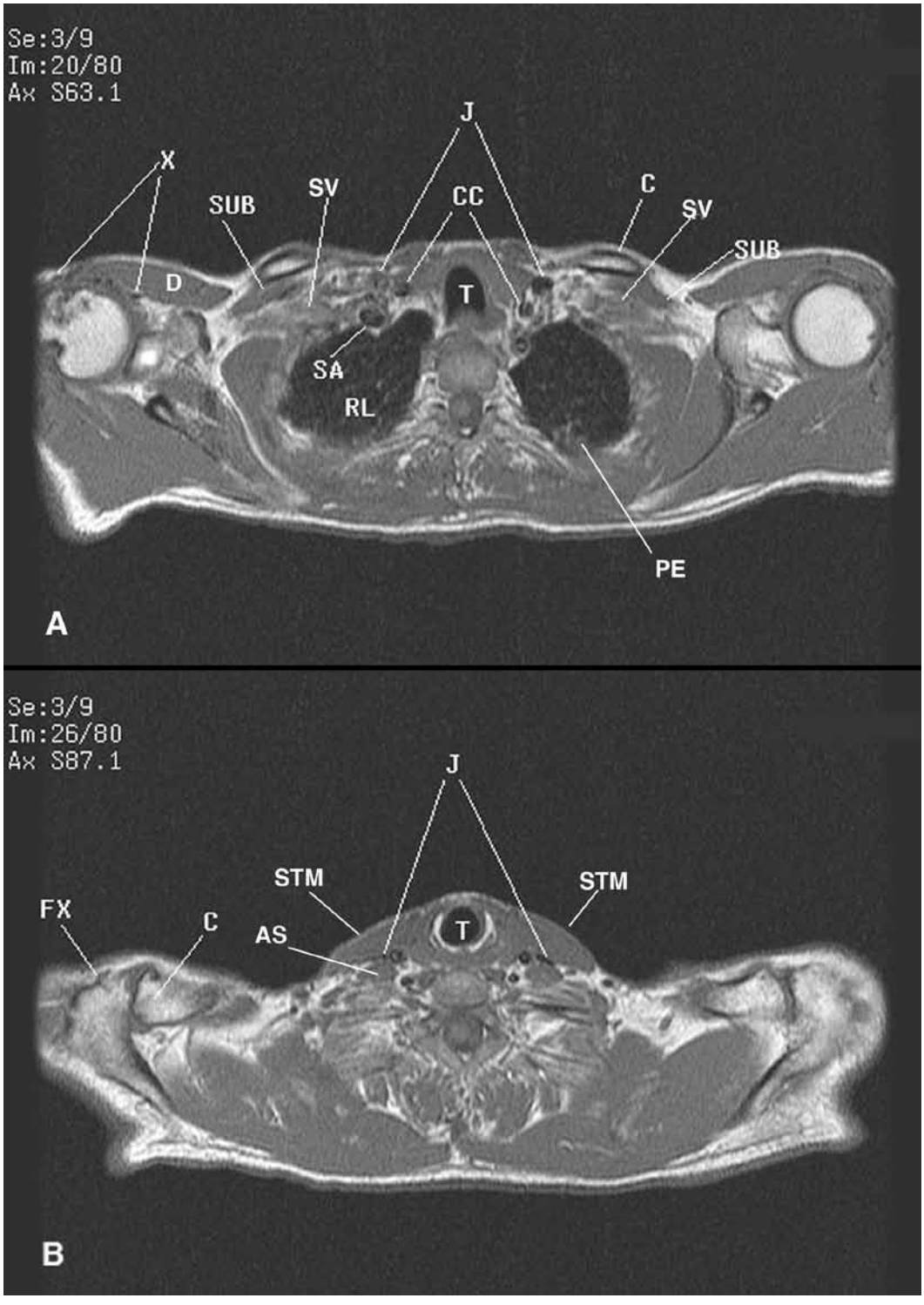

A, Image 20/80 displays the compressed inferior bicuspid valve within the right internal jugular vein (J) against the right vertebral vein (not labeled) against the first division of the right subclavian artery (SA); costoclavicular compression of the gray proton dense right subclavian vein (SV) and mild compression of the gray proton dense left subclavian vein (SV) on the first rib (unlabeled); mixed signal intensities of the screws/clips (X) marginating the scarred deltoid muscle (D), gray proton-dense pleural effusion (PE)

C indicates clavicle; CC, common carotid arteries; RL, right lung; SUB, subclavius muscle; T, trachea.

B, Image 26/80 displays fracture of the right acromion process of the scapula (FX) and bilateral Sternocleidomastoid muscle (STM) compression of the proximal internal jugular veins (J), right greater than left, against the anterior scalene muscles (AS).

C indicates distal right clavicle; T, trachea.

proton-dense left transverse cervical vein draining medial to the left external jugular vein; intermediate proximal high proton-dense left brachiocephalic vein compressed against the ascending aorta and the high proton-dense brachiocephalic trunk; high proton-dense small proximal right internal jugular vein that decreases signal intensity into the compressed decreased signal of the inferior bicuspid valve into the decreased signal of the compressed right brachiocephalic vein; high proton-dense right vertebral vein reflecting impedance to drainage as it drains into the compressed decreased signal of the right brachiocephalic vein, as compared to the small tortuous high proton-dense left vertebral vein (not displayed); dense dilated segmented proximal high proton-dense axillary veins: crimped (like a water hose) origin of the right high proton density of the brachiocephalic artery giving origin to the horizontal first division of the high proton density subclavian artery; compressed narrowing of the inferior bicuspid valve of decreased venous return within the left internal jugular vein and the compressed decreasing venous return into the brachiocephalic vein; proximal high proton density of the left brachiocephalic vein decreases signal intensity as it crosses anterior to the ascending aorta into the junction of the right brachiocephalic vein to form the superior vena cava.

Bilateral coronal abduction and external rotation of the upper extremities sequence displayed the posterior inferior rotation of the clavicles with the subclavius muscles and the posterior anterior medial rotation of the

Figure 5. Left and right T1-weighted sagittal images (38/94 and 56/94) that display hyperextension of the head and neck enfolding the overlying skin of the posterior neck (not labeled).

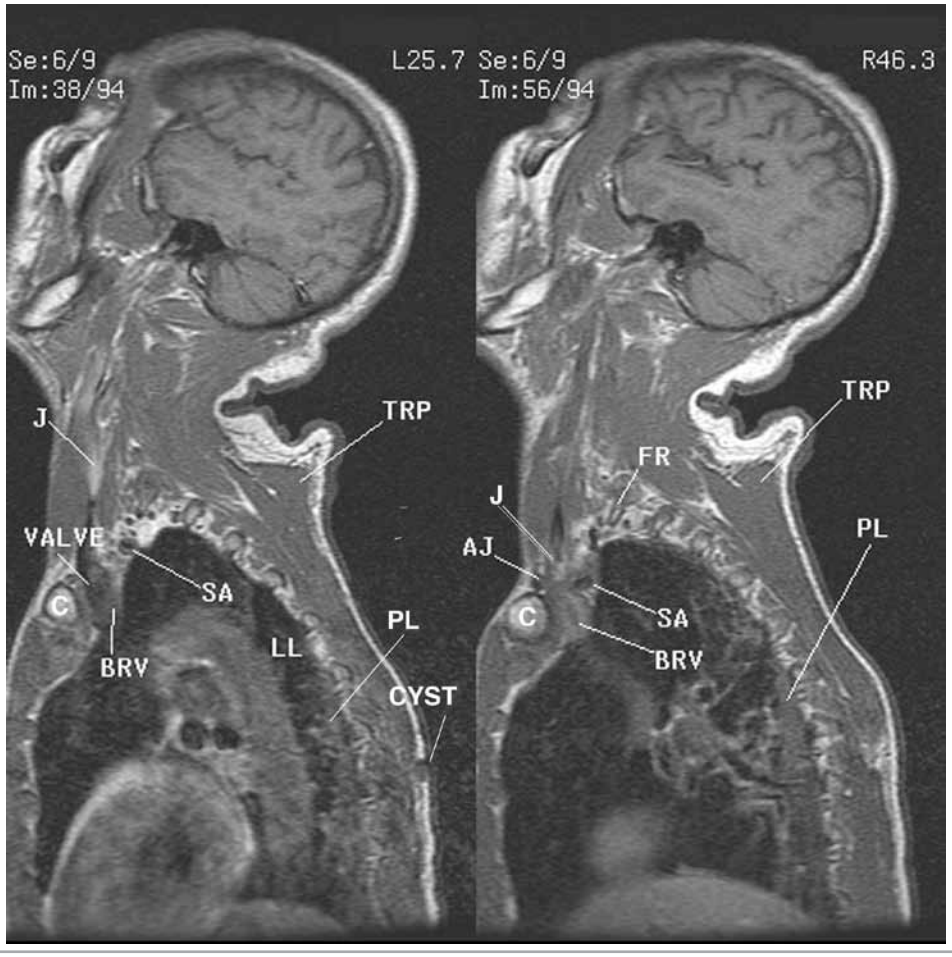

Left: Observe the gray proton dense pleural effusions over the dependent posterior lungs (PL). The left sagittal image (38/94) displays the high proton-dense proximal left internal jugular vein (J), reflecting the compression between the left sternocleidomastoid muscle and the anterior scalene muscles (not labeled); inferior bicuspid valve within the right internal jugular vein (VALVE) posterior to the anterior rotated head of the left clavicle (C) as it drains into the right gray proton-dense left brachiocephalic vein (BRV)

Right: Image 56/94 displays the anterior-rotated head of the right clavicle (C) with the valveless right anterior jugular vein (AJ) between the 2 heads of the sternocleidomastoid muscle (not labeled) compressing the inferior bicuspid valve within the right internal jugular vein (J) against the first division of the right subclavian artery (SA) as the vein and drains into the right gray proton-dense right brachiocephalic vein (BRV).

FR indicates first rib; L, left lung; PL, pleural effusion; SA, subclavian artery; TRP, trapezius muscle.

coracoid processes with attached muscles enhancing costoclavicular compression of the draining veins within the neck, supraclavicular fossae with lymphatics and compression of the subclavian and axillary arteries with binding nerves right greater than left.[3]

Bilateral abduction external rotation (AER) of the upper extremities (not displayed) captured images and triggered complaints of pain on recovery from general anesthesia. The pain was described as pinpoint over the right deltoid muscle and the anterior lateral chest wall, down the right arm with tingling and swelling of the right hand and all fingers. Left-triggered complaints consisted of pain down the forearm back and forth into the neck.

Figure 6. Three-dimensional reconstructed coronal image without contrast displays the backward displaced head and neck and high proton-dense proximal arteries and veins reflecting decreased signal intensity sites of compression displayed on the T1-weighted images of Figure 5.

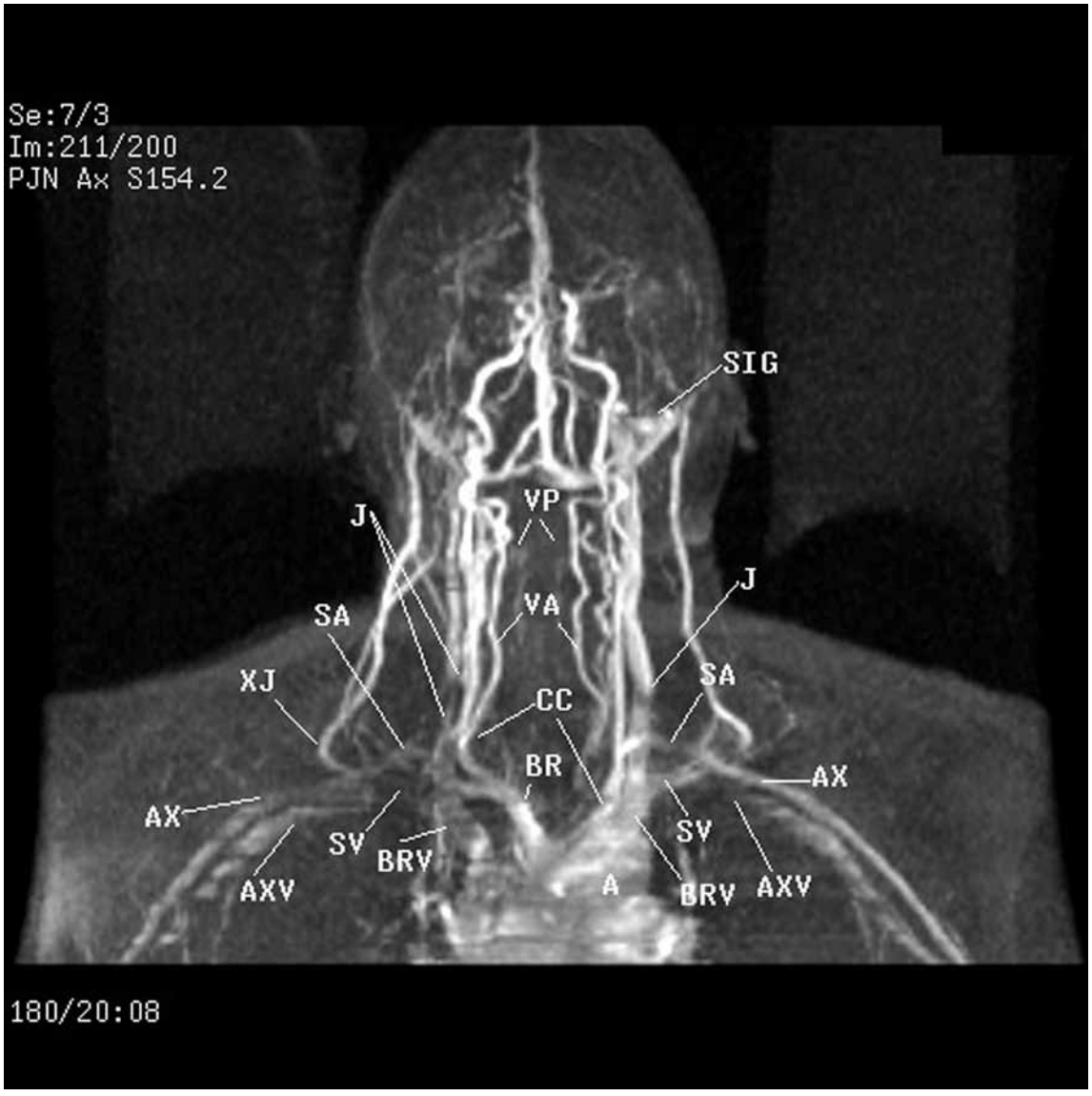

Observe the decreased signal intensity of the right small right internal jugular vein (J) as it drains compressed into the compressed right brachiocephalic vein (BRV) as compared to dominate left internal jugular vein into the left brachiocephalic vein; decreased signal intensities of the second and third divisions of the right subclavian artery (SA) and proximal right axillary artery (AX) reciprocally increasing signal intensity secondary to impedance to venous return within the compressed right subclavian vein (SV) as compared to the left axillary artery; high proton-dense turbulence within the right brachiocephalic artery (BR) reflecting impedance to arterial flow as it courses posterior to the compressed region of the inferior bicuspid valve within the right internal jugular vein; asymmetric dilated axillary veins (AXV) reflecting the asymmetric compression of the bicuspid valves within the subclavian veins (SV), and segmentation of decreased flow within the axillary veins.

A indicates aorta; CC, common carotid arteries; SIG, sigmoid sinuses; VA, vertebral arteries; VP, vertebral plexus of the spinal cord.

COMMENT

Multiplanar MRI-captured images under general anesthesia that displayed the forward shift of the cervicothoracic spine secondary to a rolled-up towel placed over the posterior neck, shoulder and back; bilateral edematous lungs with pleural effusions reflecting the impedance to venous return and lymphatic drainage in the supine position while intravenous fluids were administered; scarring and fibrosis of the superficial suprascapular nerves over the resected right anterior deltoid muscle; atrophy of the right deltoid, supraspinatus, and right serratus anterior muscles as compared to the left shoulder; ischemic fat infiltration and atrophy of the right subscapularis muscle, teres major and minor muscles; backward-displaced manubrium sloping posterior left compressing the small right internal jugular vein proximal to the inferior bicuspid valve through the compressed right medial displaced brachiocephalic vein accentuated by the dilated impedance to venous return within the right vertebral vein as compared to the dominant left internal jugular vein; marked costoclavicular compression of the right subclavian vein as compared to the left; crimped (like a water hose) brachiocephalic artery as it courses posterior to the manubrium against the trachea splaying apart the left common carotid artery as it exited the brachiocephalic trunk; serial images in the transverse sequence displaying the right sternocleidomastoid muscle compressing the smaller right internal jugular vein against the anterior scalene muscle as compared to the dominant left internal jugular vein; scarring right glenoid labrum, right anterior deltoid muscle; bilateral costoclavicular compression of the subclavian arteries and veins, right greater than left; proximal dilatation of the right axillary vein on the second rib greater than left reflecting greater impedance to venous return on the right as compared to the left; forward-rotated coracoid processes reflecting the enhanced displacement of the soft tissues posterior and also the bilateral rounding of the shoulders; right maxillary sinusitis; valveless anterior jugular veins reflecting greater diversion of venous return from the compressed right external jugular vein and subclavian veins as compared to the left, reflecting the painful right shoulder as compared to the left.

The coronal, transverse, transverse oblique, and sagittal sequence of images cross-referenced the same findings as above described, particularly the edematous lungs with effusions, crimping of the brachiocephalic artery with compression of the inferior bicuspid valve within the smaller right internal jugular vein diminishing venous return right greater than left; serial compression of the small right internal jugular vein as compared to the left.

The 2-dimensional time-of-flight MRA/MRV stacked (not displayed) and 3-dimensional reconstructed images confirmed the T1-weighted images of marked decrease in venous return within the costoclavicular compressed right subclavian vein and the subclavian artery greater than on the left.[3]

Bilateral AER coronal sequence of the upper extremities captured enhanced costoclavicular compression of the T1-weighted images, right greater than left, and on awakening from general anesthesia triggered complaints, right greater than left, as above described.

Any decrease in venous return increases intracranial, intraabdominal, and intrathoracic pressure.[6] This triggers complaints related to the 5 senses. In this case, due to general anesthesia and the impedance to posterior intercostal space expansion, the lymphatics deposited fluid in the lung and pleura.

CONCLUSIONS

- Post right rotator cuff and biceps tendon repair.
- Fibrosis and scarring of the right anterior margin of the deltoid muscle entrapping the lateral margins of the right suprascapular nerve.
- Fat infiltration secondary to the ischemic right subscapularis muscle.
- Compression of the small right internal jugular vein and right thoracic lymph duct diminished venous and lymph drainage as above described.
- Edematous lungs with pleural effusions and under general anesthesia with intravenous fluids secondary to the obstruction of the small right internal jugular vein and right thoracic lymph duct.
- Atrophy of the right serratus anterior, deltoid, trapezius, and infraspinatus muscles as above.
- Bilateral costoclavicular compression (laxity of the sling/erector muscles-trapezius, levator scapulae, and the serratus anterior muscles) of the bicuspid valves within the draining veins of the neck, supraclavicular fossae with compression of the lymphatics and compression of the subclavian arteries and axillary arteries supplying blood to the nerve of the brachial plexus and compression of the subclavian veins diminishing venous return from the same structures, right greater than left.
- Bilateral abduction external rotation of the upper extremities captured images and triggered complaints, right greater than left.

TAKE-HOME MESSAGE

The knowledge of anatomy is essential in the interpretation of plain chest radiographs. Nerves do have a blood supply.[4,5] Monitored MRI of the brachial plexus at the imaging console displayed altered fascial planes (pathology) from rotator cuff repair and obstruction to venous return at the inferior bicuspid valve in the small right internal jugular vein and compression of the right thoracic lymph duct impeding lymph flow. Since lymphatics of the lung communicate with the opposite lung, it would seem likely that fluid overload in the supine

position would be circumvented into the dependent lungs.[6] Costoclavicular compression (laxity of the sling/erector muscles) of the bicuspid valves within the draining veins of the neck and supraclavicular fossae with lymphatics diminishes venous return. Any decrease in venous return expands fascial planes and increases intrathoracic, intracranial, and intraabdominal pressures, triggering complaints of pain.[2] Intravenous fluids administered while under general anesthesia may be deposited into the soft tissues, as in our patient. Sites of obstruction in lymphedema of the arm and leg are predictable but must be confirmed by lymphography. Anesthesiologists and vascular surgeons have observed the above-described findings at the time of imaging.

REFERENCES

1. Atassoy E. Thoracic outlet compression syndrome. *Orthop Clin N Am*. 1996;27:265-303.

2. Collins JD, Saxton E, Miller TQ, Ahn S, Gelabert H, Carnes A. Scheuermann's Disease As A Model Displaying the Mechanism of Venous Obstruction in Thoracic *Outlet Syndrome and Migraine* Patients: MRI and MRA. *J Natl Med Assoc*. 2003;4:298-306.

3. Collins JD, Shaver M, Disher A, Miller TQ. The costoclavicular syndrome as displayed by MRI and MRA: Reformat and 3D graphic display. *Clin Anat*. 1997;10:131.

4. Sunderland S. Blood supply of the nerves to the upper limb in man. *Arch Neurol Psych*. 1945;53:91-115.

5. Collins JD, Shaver M, Disher A, Miller TQ. Compromising abnormalities of the brachial plexus as displayed by magnetic resonance imaging. *Clin Anat*. 1995;|8:1-16.

6. Collins JD. www.tosinfo.com. Accessed February 2011. ■